Methods

COMMUNICATION

XPS investigation of a Si-diode in operation

Sefik Suzer*

X-ray photoelectron spectroscopy (XPS) is utilized to investigate a Si-diode during its operation under both forward and reverse bias. The technique traces chemical and location specified surface potential variations as shifts of the peak positions with respect to the magnitude as well as the polarity of the applied voltage bias, which enables one to separate the dopant dependent shifts from those of the chemical ones.

Numerous powerful analytical techniques are increasingly being engaged for probing chemical, physical or electrical parameters of materials and devices under realistic operating conditions, known as *operando techniques*.[1] The majority of these techniques are photon based, like X-ray emission and absorption spectroscopy and their derivatives such as extended X-ray absorption fine structure (EXAFS), X-ray absorption near-edge structure (XANES), infra-red, Raman, sum-frequency generation, *etc.*[2–17] Particle based techniques, like Auger electron spectroscopy (AES) or X-ray photoelectron spectroscopy (XPS) and secondary ion mass spectrometry (SIMS), require a high vacuum environment, hence their utilization has not been extensive. Separately, the conventional scanning probe techniques, such as atomic force microscopy, scanning tunneling microscopy, Kelvin probe, *etc.*, provide excellent spatial resolution for electrical characterizations but do not have any chemical specificity, which is an important drawback. In this respect, in addition to the powerful elemental and chemical specificity of the electron spectroscopic techniques (AES and XPS), their ability to reflect the electrical potential of the medium surrounding the probed atom, created intentionally or not,[18–26] renders them even more powerful for investigating device performances under operational conditions. Electrical potential variations across a working device were first reported using AES three decades ago, but the technique has not been pursued due to its limited chemical specificity.[27–31] There have also been many attempts to probe potential variations across a working p–n junction device using PEEM (photoemission electron microscopy), a variant of electron spectroscopy, which also has limited chemical specificity.[32]

New and exciting applications towards investigating devices under more realistic operational conditions are now being reported as a consequence of the recent advances in ambient-pressure XPS (APXPS).[33–37] At the same time, recent advances in commercial XPS

instrumentation, like micro-focusing and parallel detection systems, have also provided new possibilities to record XPS data with higher lateral resolution in either line-scan or areal mapping modes with good statistics and in reasonable times.[38] In a recent publication, we presented an XPS investigation of a CdS-based photoresistor, taking advantage of these instrumentation capabilities, under working conditions for the device.[39] The electrical potential variations across the photoresistor were mapped by recording the Cd 3d peaks with and without illumination with different lasers to extract electrical parameters. Furthermore, morphological defects affecting the performance of the device and their response to different light sources were also determined in a chemically specific fashion. The present contribution is a continuation of our efforts, where now the p–n junction of a commercial Si-diode is investigated during its operation under forward and reverse bias. The p–n junction was chosen as the simplest representative unit of modern electronic and photovoltaic devices.[40]

A commercially available Si-diode (1N 4007) was studied after mechanically removing the protective polymer coating and a Thermo Fisher K-Alpha electron spectrometer with monochromatic AlKα X-rays was used for the XPS analysis. The instrument is slightly modified to allow imposition of an external voltage across the sample during data acquisition.[41–43] Mechanical removal of the polymeric coating left a substantial amount of organic material, most of which was cleaned by sputtering with a (1 keV) Ar$^+$ ion-gun several times. Even in the cleanest samples C and O peaks were still present in the
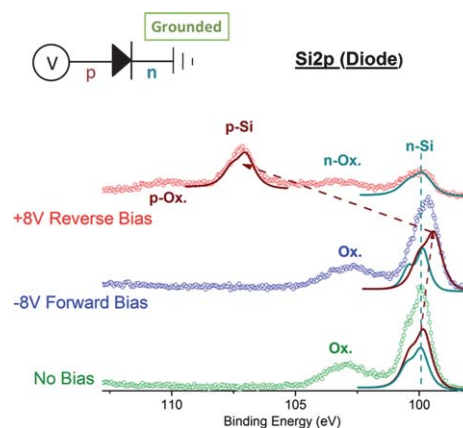

Fig. 1 The Si 2p region of the p–n junction of a Si-diode recorded under: no bias, −8 V forward and +8 V reverse bias. The inset schematically displays the electrical connection.

Department of Chemistry, Bilkent University, 06800 Ankara, Turkey. E-mail: suzer@fen.bilkent.edu.tr
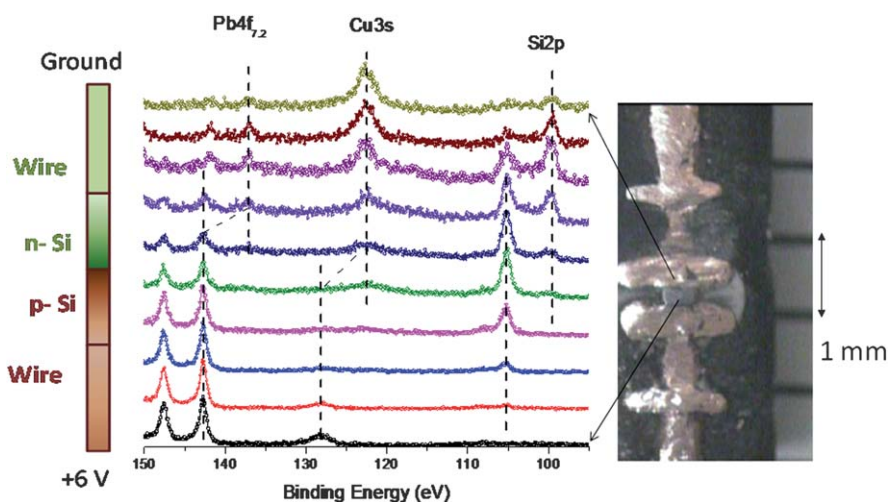
Fig. 2 An extended region of the same device recorded in a line-scan mode with 100 μm spot size and at 30 μm steps, covering all together 300 μm across the p–n junction under +6 V reverse bias. Spectral features of the connecting wires are also visible and follow faithfully the voltage variations. A picture of the device and the analysed region is also given as an inset.

survey spectra but did not interfere with the measurements to be presented. For survey scans, an X-ray beam size of 400 μm was used, but for the data presented in this work, a 100 μm diameter X-ray spot size was used both in recording the regions as well as in the line scans with 30 to 100 μm steps in between the data points.

In Fig. 1 we display the Si 2p region of a 100 μm spot size on the junction, positioned approximately in the very middle, under different bias conditions, where the diode was grounded from the n-

side and the potential was applied from the p-side. This mode of connection was preferred in order not to disturb the flood-gun operation since parts of the sample covered with the polymer residues were charging, but grounding the p-side and applying the bias from the n-side also gave similar results.

When no bias is applied, we observe one metallic (Si^0) peak and one oxide (Si^{X+}) peak. The metallic peak is deconvoluted into two spin–orbit doublets with the theoretical 0.608 eV splitting and
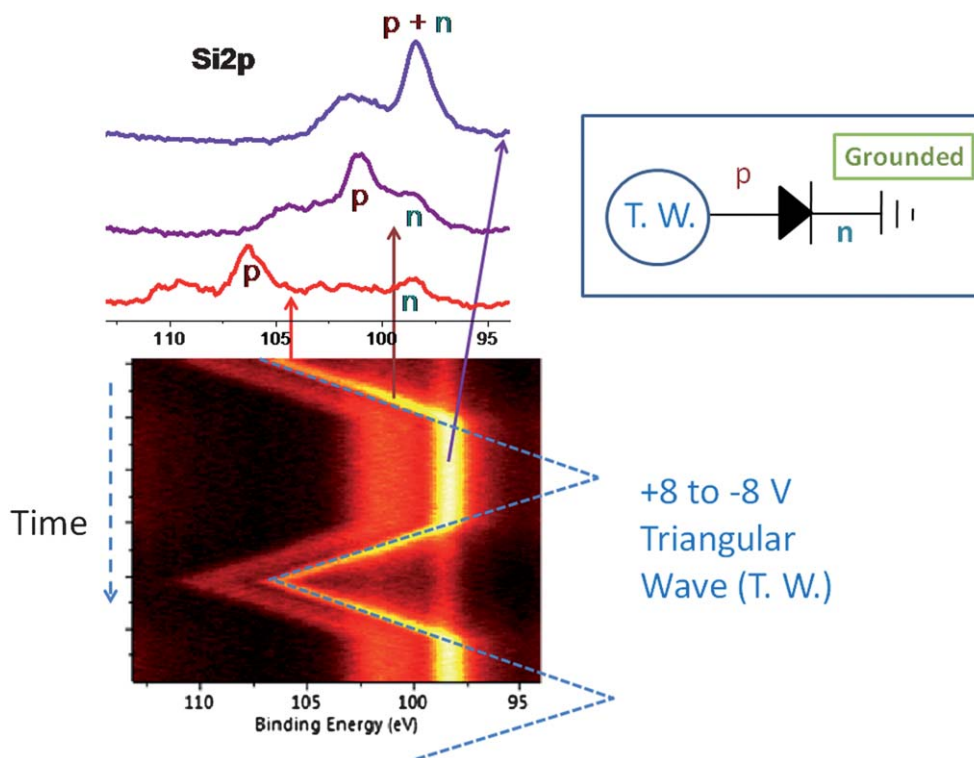

Fig. 3 The Si 2p region of the device recorded in the 2 s snapshots while subjecting it to a +8 V to −8 V triangular wave excitation with a repetition rate of 1000 s. The inset on the left side displays the spectra in the conventional way at positions corresponding to +8 V, +5 V and −8 V bias, respectively. The inset on the right side is a schematic of the operation.

assigned to p-Si and n-Si components at more or less the same binding energy of 99.8 eV. Under −8 V forward bias, the Si⁰ feature becomes broader but can again be fitted into an n-component, not shifted, and to a p-component, shifted down by *ca.* −0.5 eV. The most dramatic splitting is observed under +8 V reverse bias, where, although again the n-component is not shifted, the p-component is exactly +8 eV up-shifted in the binding energy scale. As can be gathered from the figure, the oxide peak is also split and up-shifted accordingly.

Fig. 2 displays a larger energy window spectra recorded in the line-scan mode with 30 μm steps across the p–n junction under +6 V reverse bias, where not only the Si 2p but also the Cu 3s and the Pb 4f peaks of the connecting wires faithfully display the position dependent shifts. Since the lateral resolution is only 100 μm, which is not sufficient to distinguish the n-side from the p-side, we are sampling both sides of the junction. Hence, all peaks are doubled, when an area consisting both p- and n-regions, traversing the junction.

Similar to recording the *I–V* characteristics of a diode, triangular wave excitation can also be utilized to record the peak positions as a function of the applied voltage. As shown in Fig. 3 for the same Si 2p region, recorded now in the 2 second long snap-shot mode with somewhat poorer energy resolution, the spectral features are faithfully reproduced, and a sharp cut-off voltage is clearly visible, representing the *perfect rectifying action* of the diode. The repetition rate was 1000 s for the data presented in the figure, but faster scans (not shown) up to 0.1 Hz dependably reflect all of the spectral features investigated as well as the rectifying action of the device. However, for recording the data under faster voltage variations, a different form of data gathering, like application of square-wave excitation, is more informative.[37]

Conclusions

We have demonstrated that a contactless chemical and electrical measurement of a Si-diode, representing a p–n junction, can be performed under realistic working conditions using XPS, where under the reverse bias, the applied potential is directly translated to the peak positions of the p-Si side and the connecting wire. Other spectral features of the surface domains exhibit similar behavior. In addition, time dependent (a.c.) behavior is extracted by imposing a triangular bias voltage form with various frequencies while recording XPS data to reveal the rectification action of the diode. These simple variations introduce a new dimension to the well-utilized surface and chemically sensitive XPS technique for extracting chemically specific electrical information towards investigating and/or assessing performance of devices under operating conditions in a non-contact fashion. Our methodology opens a new dimension of analyzing electrical characteristics of devices, which is simple to implement, and the derived chemically resolved electrical parameters can be used to assess the performance of devices and/or to detect and identify the nature of malfunctioning and/or defect sites in a chemically specific fashion.

Acknowledgements

References

1 A. Gurlo and R. Riedel, *Angew. Chem., Int. Ed.*, 2007, **46**, 3826.
2 B. Coq, G. Delahay, R. Durand, D. Berthomieu and E. Ayala-Villagomez, *J. Phys. Chem. B*, 2004, **108**, 11062.
3 A. F. Lee, P. Carr and K. Wilson, *J. Phys. Chem. B*, 2004, **108**, 14811.
4 M. O. Guerrero-Pérez and M. A. Bañares, *J. Phys. Chem. C*, 2006, **111**, 1315.
5 A. V. Whitney, J. W. Elam, P. C. Stair and R. P. Van Duyne, *J. Phys. Chem. C*, 2007, **111**, 16827.
6 M. V. Martínez-Huerta, G. Deo, J. L. G. Fierro and M. A. Bañares, *J. Phys. Chem. C*, 2008, **112**, 11441.
7 C. Zhao and I. E. Wachs, *J. Phys. Chem. C*, 2008, **112**, 11363.
8 F. Klasovsky, J. Hohmeyer, A. Brückner, M. Bonifer, J. R. Arras, M. Steffan, M. Lucas, J. R. Radnik, C. Roth and P. Claus, *J. Phys. Chem. C*, 2008, **112**, 19555.
9 R. Rousseau, G. K. Schenter, J. L. Fulton, J. C. Linehan, M. H. Engelhard and T. Autrey, *J. Am. Chem. Soc.*, 2009, **131**, 10516.
10 B. Kimmerle, J.-D. Grunwaldt, A. Baiker, P. Glatzel, P. Boye, S. Stephan and C. G. Schroer, *J. Phys. Chem. C*, 2009, **113**, 3037.
11 J. Melke, A. Schoekel, D. Dixon, C. Cremers, D. E. Ramaker and C. Roth, *J. Phys. Chem. C*, 2010, **114**, 5914.
12 D. Gamarra, M. Fernandez-Garcia, C. Belver and A. Martinez-Arias, *J. Phys. Chem. C*, 2010, **114**, 18576.
13 I. Kendrick, D. Kumari, A. Yakaboski, N. Dimakis and E. S. Smotkin, *J. Am. Chem. Soc.*, 2010, **132**, 17611.
14 J. Xu, P. Li, X. Song, C. He, J. Yu and Y.-F. Han, *J. Phys. Chem. Lett.*, 2010, **1**, 1648.
15 K. Fottinger, J. A. van Bokhoven, M. Nachtegaal and G. Rupprechter, *J. Phys. Chem. Lett.*, 2011, **2**, 428.
16 I. Laoufi, M. C. Saint-Lager, R. Lazzari, J. Jupille, O. Robach, S. Garaudée, G. Cabailh, P. Dolle, H. Cruguel and A. Bailly, *J. Phys. Chem. C*, 2011, **115**, 4673.
17 M. A. Banares, *Adv. Mater.*, 2011, **23**, 5293.
18 K. Shabtai, I. Rubinstein, S. R. Cohen and H. Cohen, *J. Am. Chem. Soc.*, 2000, **122**, 4959.
19 R. Buller, H. Cohen, E. Minkin, R. Popovitz-Biro, E. Lifshitz and M. Lahav, *Adv. Funct. Mater.*, 2002, **12**, 713.
20 A. Samokhvalov, R. W. Gurney, M. Lahav, S. Cohen, H. Cohen and R. Naaman, *J. Phys. Chem. B*, 2003, **107**, 4245.
21 H. Cohen, R. Maoz and J. Sagiv, *Nano Lett.*, 2006, **6**, 2462.
22 H. Cohen, S. K. Sarkar and G. Hodes, *J. Phys. Chem. B*, 2006, **110**, 25508.
23 S. K. Sarkar, G. Hodes, L. Kronik and H. Cohen, *J. Phys. Chem. C*, 2008, **112**, 6564.
24 R. J. Phaneuf, H. C. Kan, M. Marsi, L. Gregoratti, S. Gunther and M. Kiskinova, *J. Appl. Phys.*, 2000, **88**, 863.
25 L. Gregoratti, T. O. Mentes, A. Locatelli and M. Kiskinova, *J. Electron Spectrosc. Relat. Phenom.*, 2009, **170**, 13.
26 N. Barrett, L. F. Zagonel, O. Renault and A. Bailly, *J. Phys.: Condens. Matter*, 2009, **21**, 314015.
27 R. Pantel, *Appl. Phys. Lett.*, 1983, **43**, 650.
28 J. M. Patterson and M. C. Smith, *21st Annual Proceedings, Reliability Physics 1983, Phoenix, AZ, April 5–7, 1983, Institute of Electrical and Electronics Engineers (IEEE)*, New York, 1983, p. 150.
29 R. B. Comizzoli and R. L. Opila, *J. Appl. Phys.*, 1987, **61**, 261.
30 R. L. Opila, L. Marchut and J. N. Hollenhorst, *J. Electrochem. Soc.*, 1990, **137**, 703.
31 R. L. Opila, *Appl. Surf. Sci.*, 2009, **256**, 1313.
32 M. Giesen, R. J. Phaneuf, E. D. Williams, T. L. Einstein and H. Ibach, *Appl. Phys. A: Mater. Sci. Process.*, 1997, **64**, 423.
33 S. Ghosal, J. C. Hemminger, H. Bluhm, B. S. Mun, E. L. D. Hebenstreit, G. Ketteler, D. F. Ogletree, F. G. Requejo and M. Salmeron, *Science*, 2005, **307**, 563.
34 H. Bluhm, *J. Electron Spectrosc. Relat. Phenom.*, 2010, **177**, 71.
35 F. El Gabaly, M. Grass, A. H. McDaniel, R. L. Farrow, M. A. Linne, Z. Hussain, H. Bluhm, Z. Liu and K. F. McCarty, *Phys. Chem. Chem. Phys.*, 2010, **12**, 12138.
36 C. Zhang, M. E. Grass, A. H. McDaniel, S. C. DeCaluwe, F. El Gabaly, Z. Liu, K. F. McCarty, R. L. Farrow, M. A. Linne and Z. Hussain, *Nat. Mater.*, 2010, **9**, 944.
37 F. Tao, *Chem. Commun.*, 2012, **48**, 3812.

38 B. Pelissier, A. Beaurain, J. P. Barnes, R. Gassilloud, F. Martin and O. Joubert, *Microelectron. Eng.*, 2008, **85**, 1882.

39 H. Sezen, A. A. Rockett and S. Suzer, *Anal. Chem.*, 2012, **84**, 2990.

40 H. Sezen and S. Suzer, *J. Chem. Phys.*, 2011, **135**, 141102.

41 H. Sezen and S. Suzer, *Surf. Sci.*, 2010, **604**, L59.

42 H. Sezen, E. Ozbay, O. Aktas and S. Suzer, *Appl. Phys. Lett.*, 2011, **98**, 111901.

43 H. Sezen, S. Suzer and A. Dana, *Anal. Chem.*, 2008, **80**, 3931.